

## Supporting information

### Aluminum complexes based on pyridine substituted alcohols: synthesis, structure, catalytic application in ROP

Marina M. Kireenko,<sup>a</sup> Ekaterina A. Kuchuk,<sup>a</sup> Kirill V. Zaitsev,<sup>a,\*</sup> Viktor A. Tafeenko,<sup>a</sup> Yuri F. Oprunenko,<sup>a</sup> Andrei V. Churakov,<sup>b</sup> Elmira Kh. Lermontova,<sup>b</sup> Galina S. Zaitseva<sup>a</sup> and Sergey S. Karlov<sup>a</sup>

<sup>a</sup>Chemistry Department, Moscow State University, B-234 Leninskie Gory, 119991 Moscow, Russia

<sup>b</sup>Institute of General and Inorganic Chemistry, Russian Acad. Sci., Leninskii pr., 31, 119991 Moscow, Russia

E-mail: zaitsev@org.chem.msu.ru

### Table of Contents

<b>Fig. S1</b> <sup>1</sup> H NMR spectrum for <b>3a</b> (CDCl <sub>3</sub> , rt)	S3
<b>Fig. S2</b> <sup>1</sup> H NMR spectrum for <b>3a</b> (CDCl <sub>3</sub> + 20 % DMSO-d6, rt)	S3
<b>Fig. S3</b> DOSY NMR spectrum for <b>3a</b> and calculation of M <sub>w</sub>	S4
<b>Fig. S4</b> Molecular structure of complex <b>2c</b>	S6
<b>Fig. S5.</b> MALDI-TOF mass spectrum of a PLA sample prepared with <b>2a</b>	S6
<b>Fig. S6.</b> <sup>1</sup> H NMR spectra (CDCl <sub>3</sub> ) for BnO-PLLA, prepared with <b>2a</b> (75 % conversion)	S7
<b>Fig. S7.</b> <sup>1</sup> H NMR spectra (CDCl <sub>3</sub> ) for MeO-PLLA, prepared with <b>2c</b> (100 % conversion)	S8
<b>Fig. S8.</b> Homodecoupled <sup>1</sup> H NMR spectra (CDCl <sub>3</sub> ) for BnO-PLLA	S8
<b>Fig. S9.</b> ln([LA] <sub>0</sub> /[LA]) versus time plot for <i>L</i> -lactide polymerization with <b>2a-4a</b>	S9
<b>Fig. S10.</b> M <sub>n</sub> versus conversion plot for <i>L</i> -lactide polymerization with <b>3a</b>	S9

<b>Fig. S11.</b> $\text{Ln}([\text{M}]_0/[\text{M}])$ vs. time plots for the polymerization of <i>L</i> -lactide in the presence of catalytic complex <b>4a</b>	S10
<b>Fig. S12.</b> $^1\text{H}$ NMR spectrum ( $\text{CDCl}_3$ , rt) for PLLA (the sample contains the polymer, [( <b>3</b> )(PLLA)], with ligand fragment)	S10
<b>Figure S13.</b> $^1\text{H}$ NMR spectrum ( $\text{CDCl}_3$ , rt) of complex <b>2a</b>	S11
<b>Figure S14.</b> $^{13}\text{C}$ NMR spectrum ( $\text{CDCl}_3$ , rt) of complex <b>2a</b>	S11
<b>Figure S15.</b> $^1\text{H}$ NMR spectrum ( $\text{CDCl}_3$ , rt) of complex <b>3a</b>	S12
<b>Figure S16.</b> $^{13}\text{C}$ NMR spectrum ( $\text{CDCl}_3$ , rt) of complex <b>3a</b>	S12
<b>Figure S17.</b> $^1\text{H}$ NMR spectrum ( $\text{CDCl}_3$ , rt) of complex <b>4a</b>	S13
<b>Figure S18.</b> $^{13}\text{C}$ NMR spectrum ( $\text{CDCl}_3$ , rt) of complex <b>4a</b>	S13
<b>Figure S19.</b> $^{13}\text{C}$ NMR spectrum ( $\text{CDCl}_3$ , rt) of complex <b>3b</b>	S14
<b>Figure S20.</b> $^{13}\text{C}$ NMR spectrum ( $\text{CDCl}_3$ , rt) of complex <b>3b</b>	S14
<b>Figure S21.</b> $^1\text{H}$ NMR spectrum ( $\text{CDCl}_3$ , rt) of complex <b>4b</b>	S15
<b>Figure S22.</b> $^{13}\text{C}$ NMR spectrum ( $\text{CDCl}_3$ , rt) of complex <b>4b</b>	S15
<b>Figure S23.</b> $^1\text{H}$ NMR spectrum ( $\text{CDCl}_3$ , rt) of complex <b>2c</b>	S16
<b>Figure S24.</b> $^{13}\text{C}$ NMR spectrum ( $\text{CDCl}_3$ , rt) of complex <b>2c</b>	S16
<b>Figure S25.</b> $^1\text{H}$ NMR spectrum ( $\text{CDCl}_3$ , rt) of complex <b>3c</b>	S17
<b>Figure S26.</b> $^{13}\text{C}$ NMR spectrum ( $\text{CDCl}_3$ , rt) of complex <b>3c</b>	S17
<b>Figure S27.</b> $^1\text{H}$ NMR spectrum ( $\text{CDCl}_3$ , rt) of complex <b>4c</b>	S18
<b>Figure S28.</b> $^1\text{H}$ NMR spectrum ( $\text{C}_6\text{D}_6$ , rt) of complex <b>2d</b>	S18
<b>Figure S29.</b> $^{13}\text{C}$ NMR spectrum ( $\text{C}_6\text{D}_6$ , rt) of complex <b>2d</b>	S19

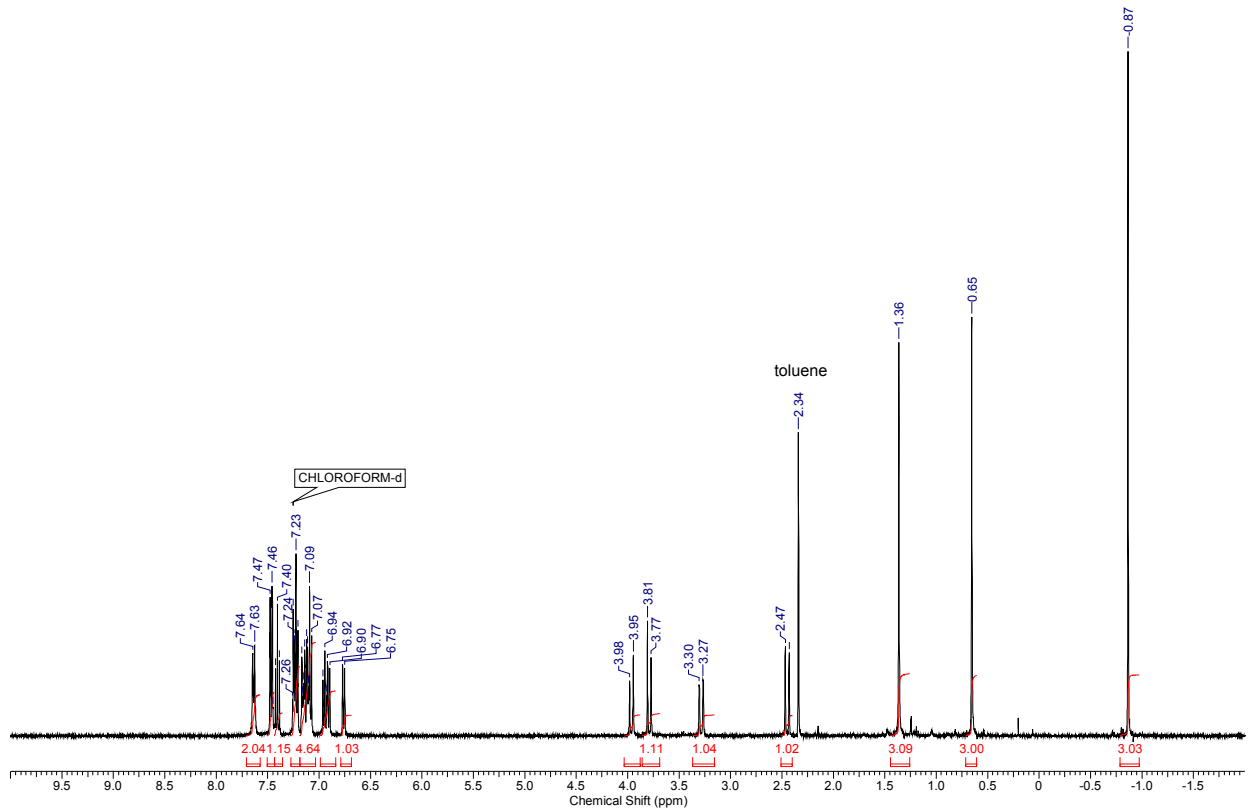


**Fig. S1**  $^1\text{H}$  NMR spectrum for **3a** ( $\text{CDCl}_3$ , rt).

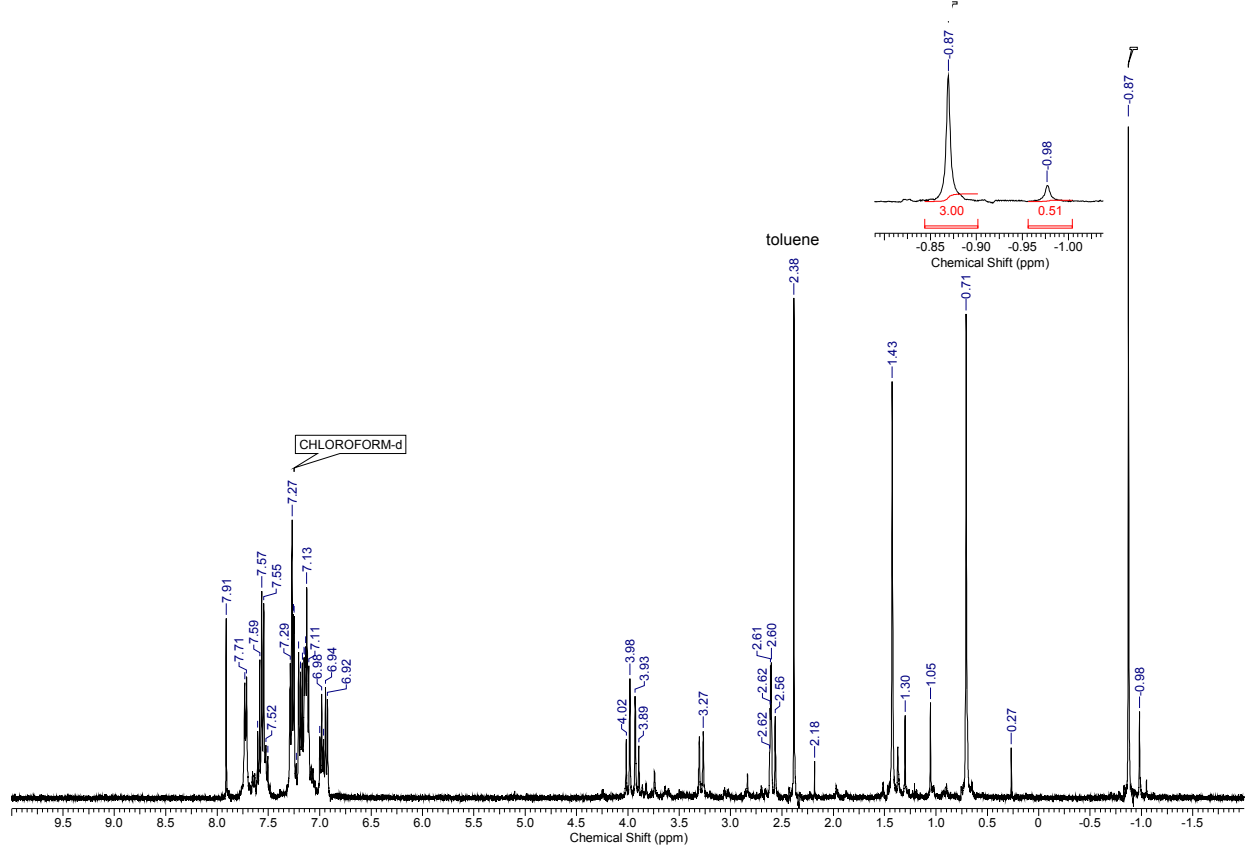


**Fig. S2**  $^1\text{H}$  NMR spectrum for **3a** ( $\text{CDCl}_3 + 20\%$   $\text{DMSO-d}_6$ , rt).

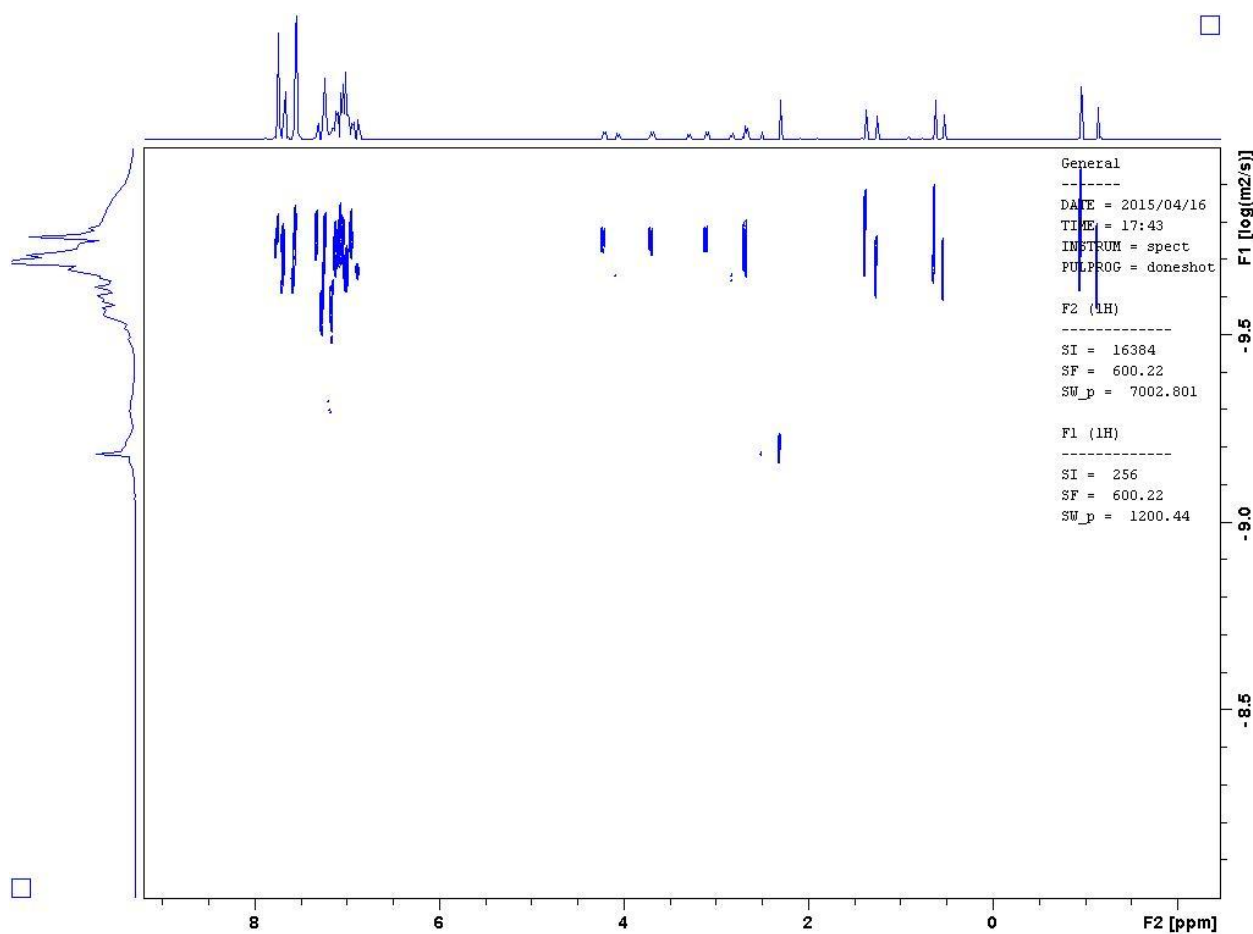


**Fig. S3** DOSY NMR spectrum for **3a** (600 MHz, DMSO-d<sub>6</sub>, room temperature; the admixture of toluene is present).

The formula of MW calculation [*Angew. Chem., Int. Ed.* 2013, **52**, 3199 – 3202]

$$D = \frac{k_B T \left( \frac{3\alpha}{2} + \frac{1}{1+\alpha} \right)}{6\pi\eta_3 \sqrt{\frac{3MW}{4\pi\rho_{eff} N_A}}}, \text{ where}$$

$$\alpha = \sqrt[3]{\frac{MW_s}{MW}}$$

MW<sub>S</sub> – molecular weight of the solvent

MW – molecular weight of the solute

$\rho_{eff}$  - the effective density of a small molecule

$\eta$ -viscosity

$N_A$  - the Avogadro number

$k_B$  - Boltzmann constant

D – diffusion coefficient

T - temperature

Using known calculation algorithm the molecular weights of two particles was established:

$M_1 = 820 \text{ g/mol}$ ,  $D = 1.74 \times 10^{-10} \text{ m}^2/\text{s}$  ( $M_1(\text{theor}) = 774.9$ ), what corresponds to dimeric **(3a)<sub>2</sub>**;

$M_2 = 497.1 \text{ g/mol}$ ,  $D = 2.19 \times 10^{-10} \text{ m}^2/\text{s}$  ( $M_1(\text{theor}) = 465.6$ ), what corresponds to adduct of monomer with DMSO.

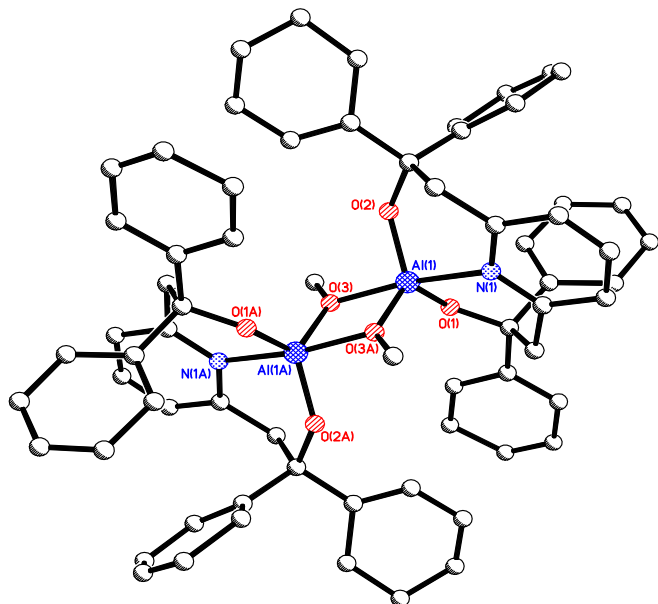


**Fig. S4** Molecular structure of complex **2c**. Hydrogen atoms are omitted for clarity.

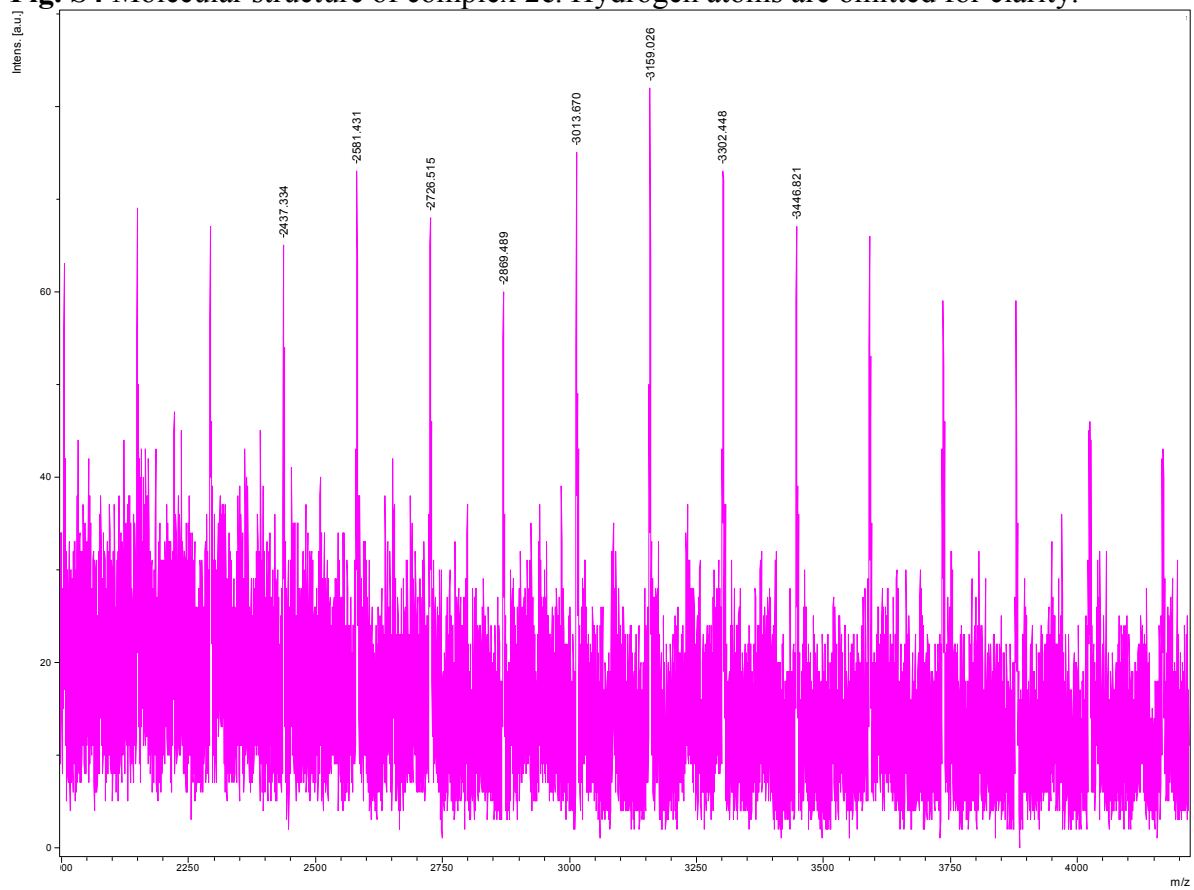


**Fig. S5.** MALDI-TOF mass spectrum of a PLA sample prepared with **2a** (Table 2, entry 1) (solvent THF, HABA matrix, 2,5-dihydroxybenzoic acid).

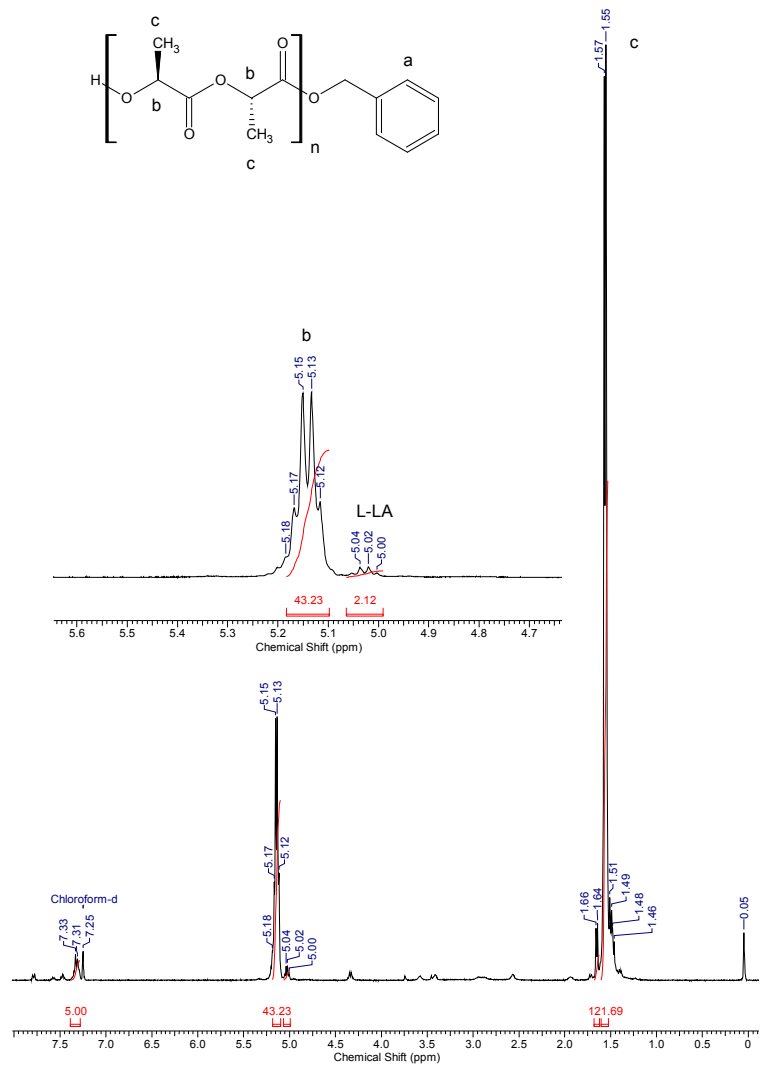


**Fig. S6.**  $^1\text{H}$  NMR spectra (CDCl<sub>3</sub>) for BnO-PLLA, prepared with **2a** (75 % conversion).

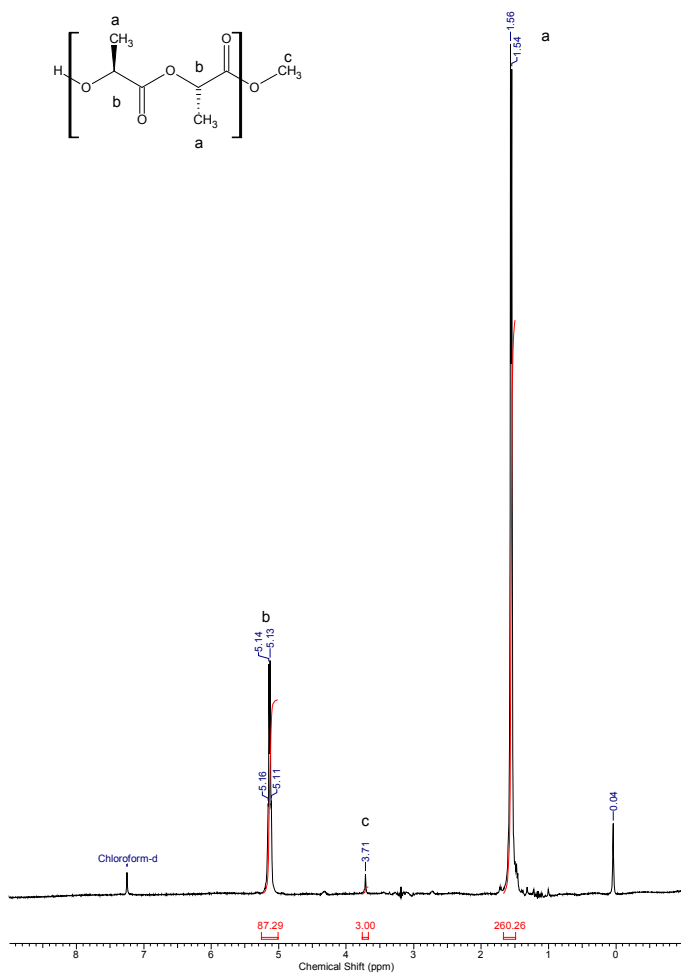


**Fig. S7.**  $^1\text{H}$  NMR spectra ( $\text{CDCl}_3$ ) for MeO-PLLA, prepared with **2c** (100 % conversion).

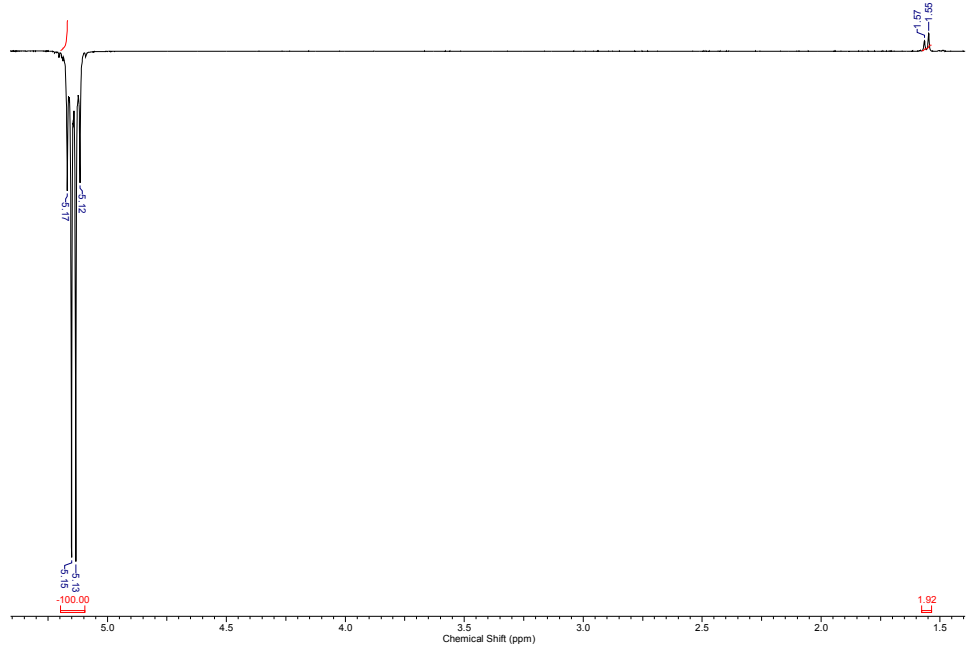


**Fig. S8.** Homodecoupled  $^1\text{H}$  NMR spectra ( $\text{CDCl}_3$ ) for BnO-PLLA.

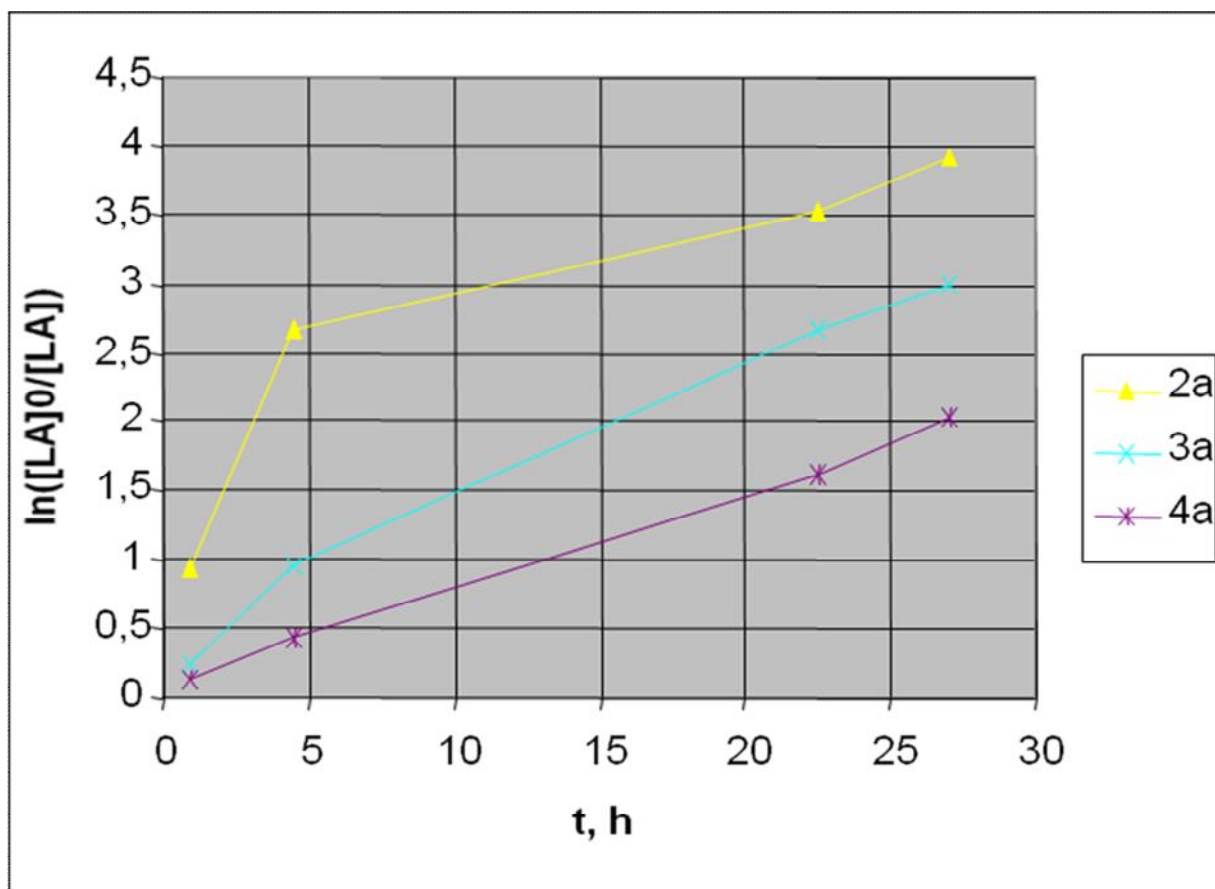


**Fig. S9.**  $\ln([LA]_0/[LA])$  versus time plot for *L*-lactide polymerization with **2a-4a**.

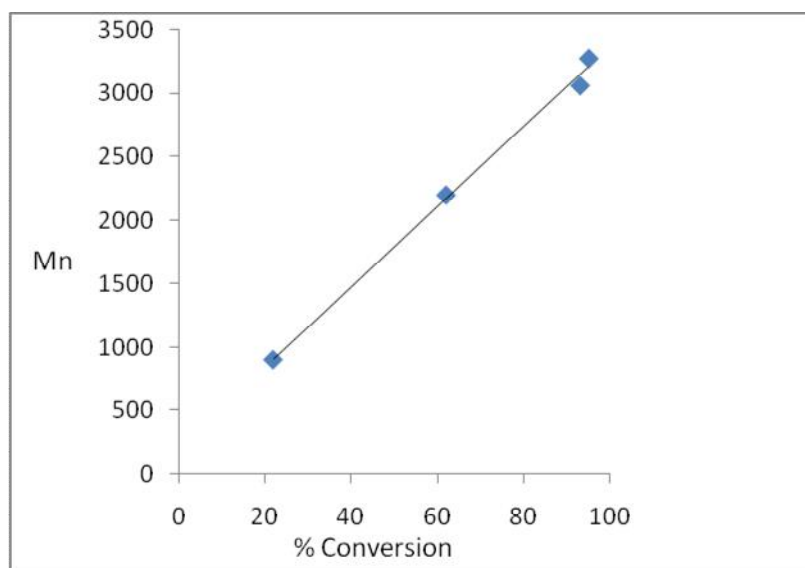


**Fig. S10.**  $M_n$  versus conversion plot for *L*-lactide polymerization with **3a**.

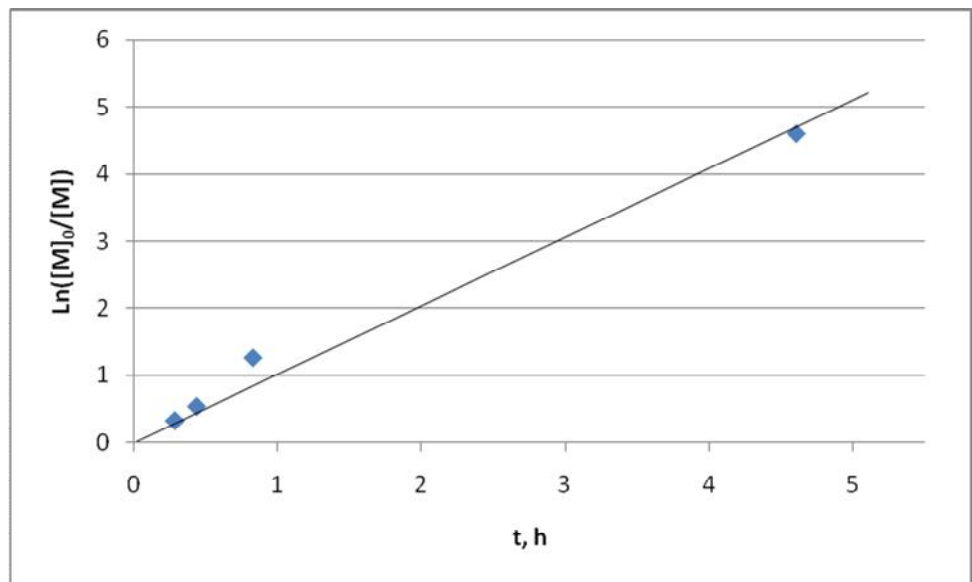


**Fig. S11.**  $\ln([M]_0/[M])$  vs. time plots for the polymerization of *L*-lactide in the presence of catalytic complex **4a** (100:1:1) at 80 °C; [LA]/[initiator]= 100.

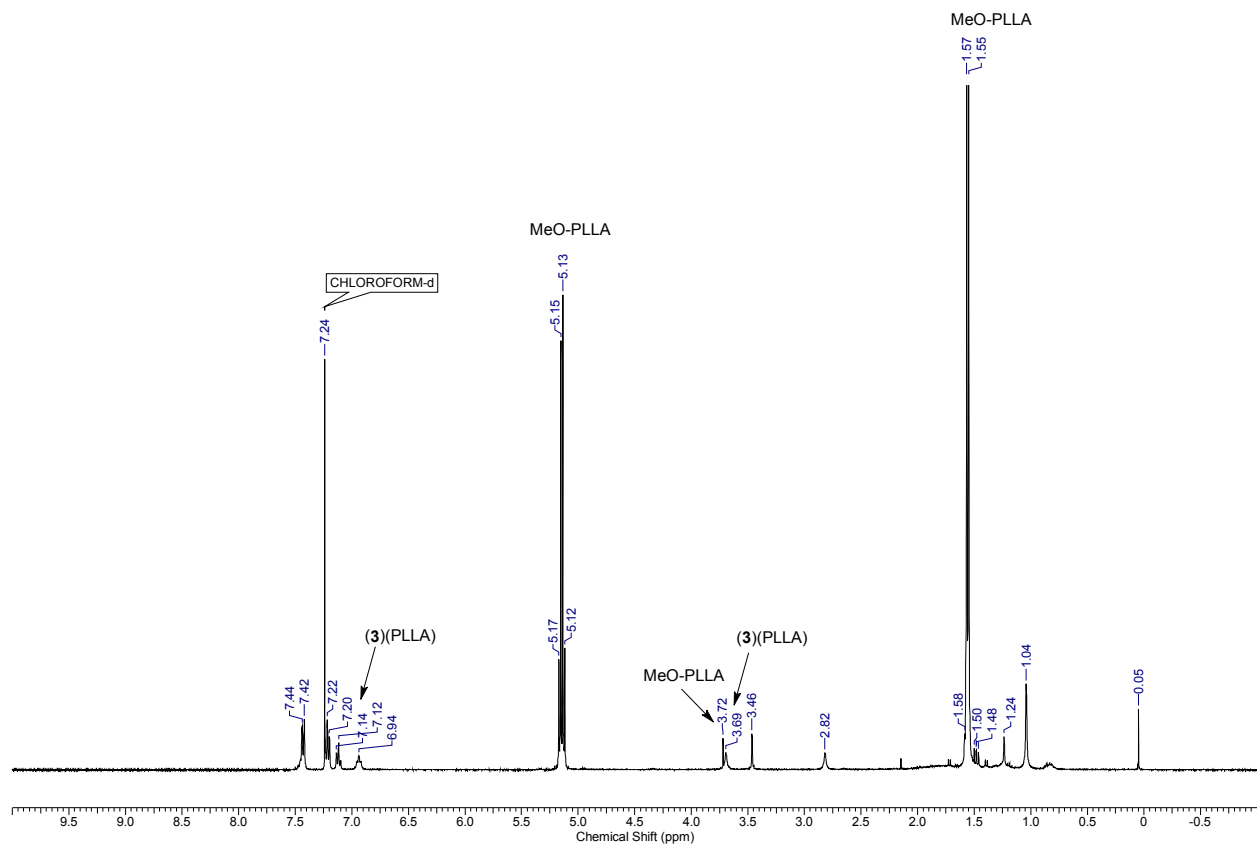


**Fig. S12.**  $^1\text{H}$  NMR spectrum ( $\text{CDCl}_3$ , rt) for PLLA (the sample contains the polymer,  $[(3)(\text{PLLA})]$ , with ligand fragment).

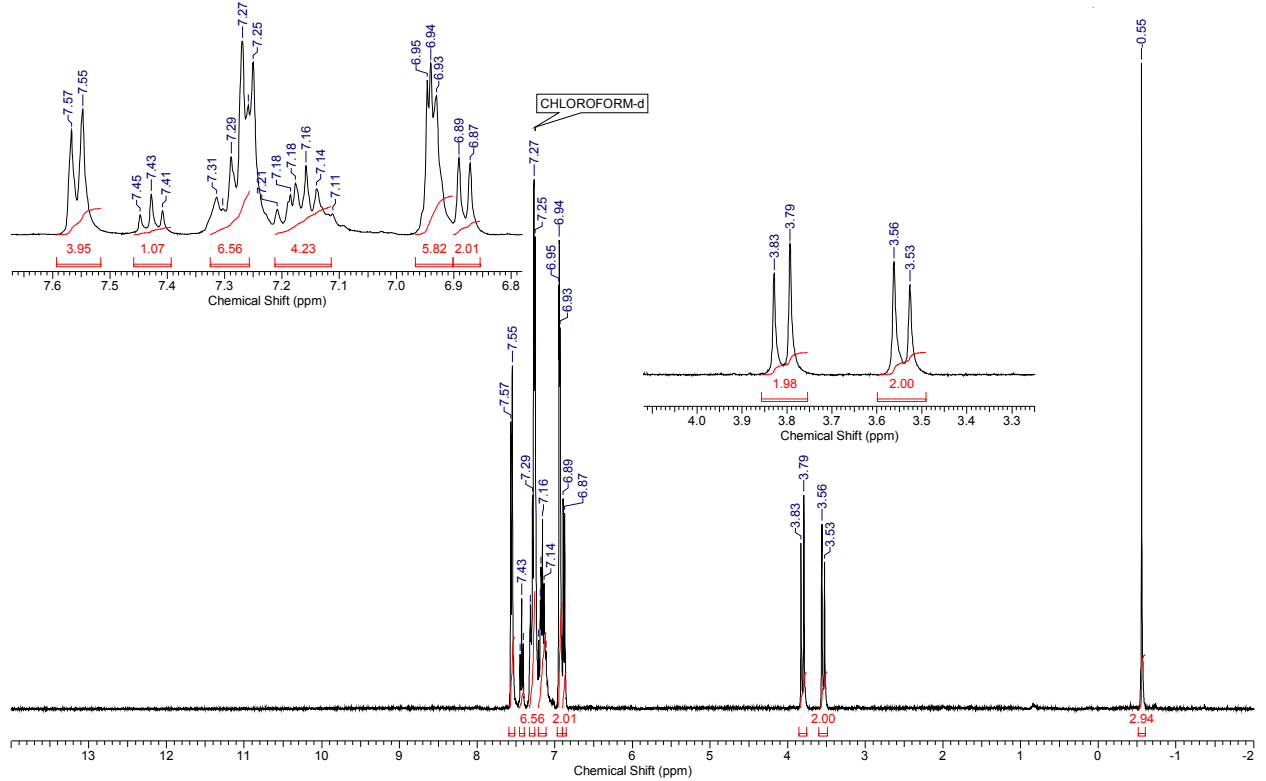


**Figure S13.**  $^1\text{H}$  NMR spectrum ( $\text{CDCl}_3$ , rt) of complex **2a**.

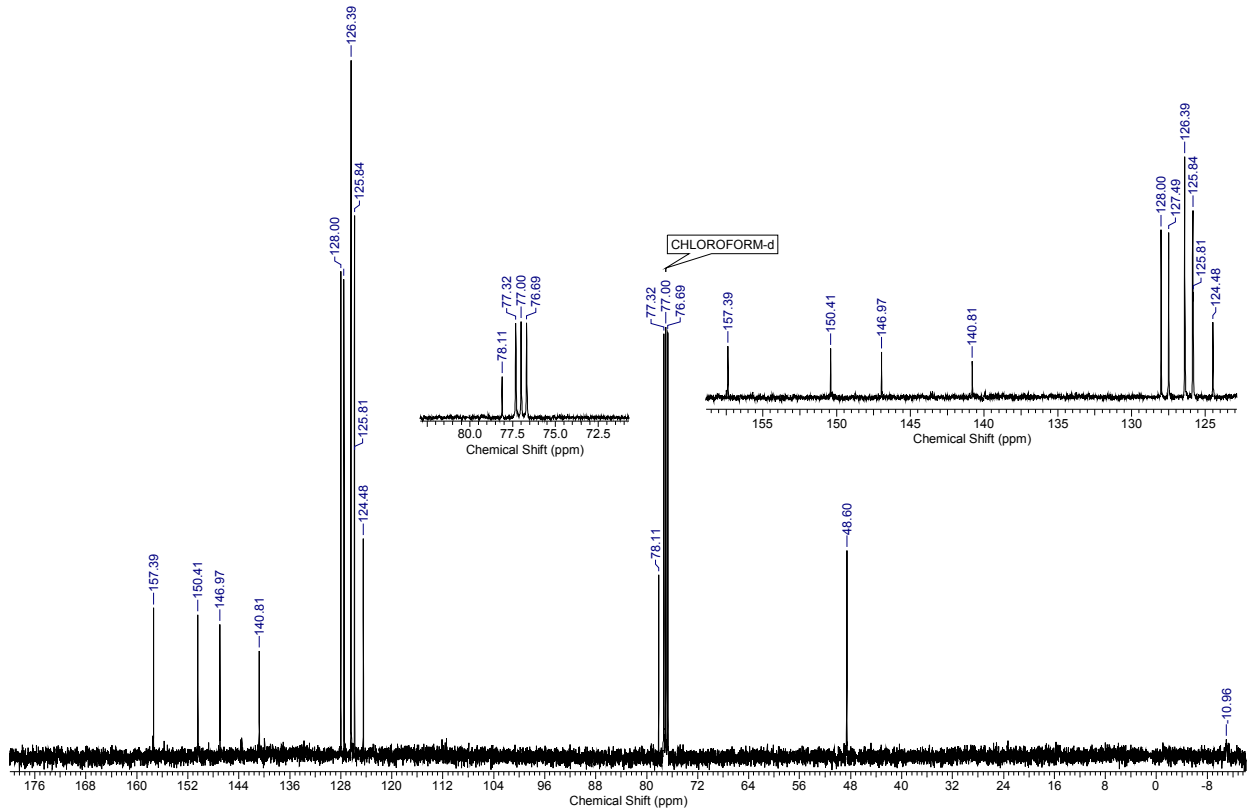


**Figure S14.**  $^{13}\text{C}$  NMR spectrum ( $\text{CDCl}_3$ , rt) of complex **2a**.

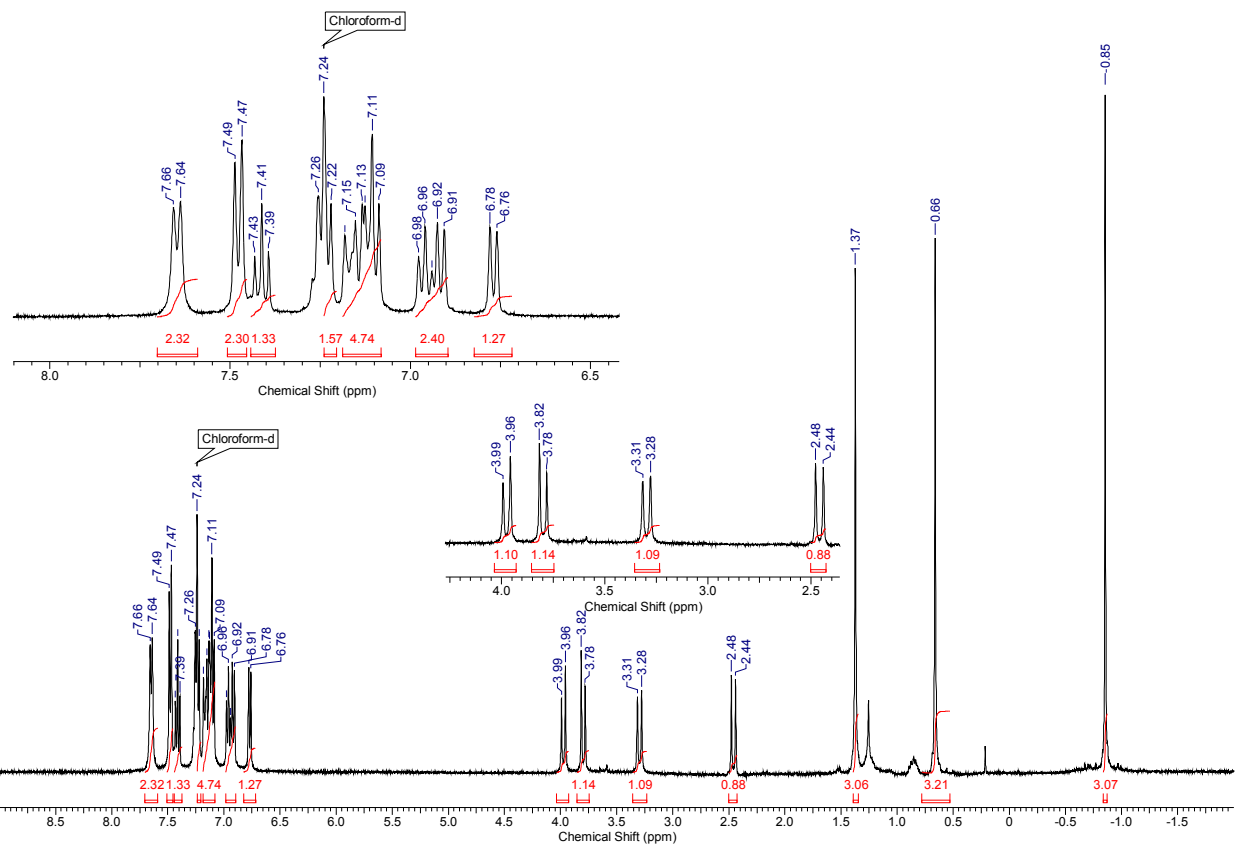


**Figure S15.** <sup>1</sup>H NMR spectrum (CDCl<sub>3</sub>, rt) of complex 3a.

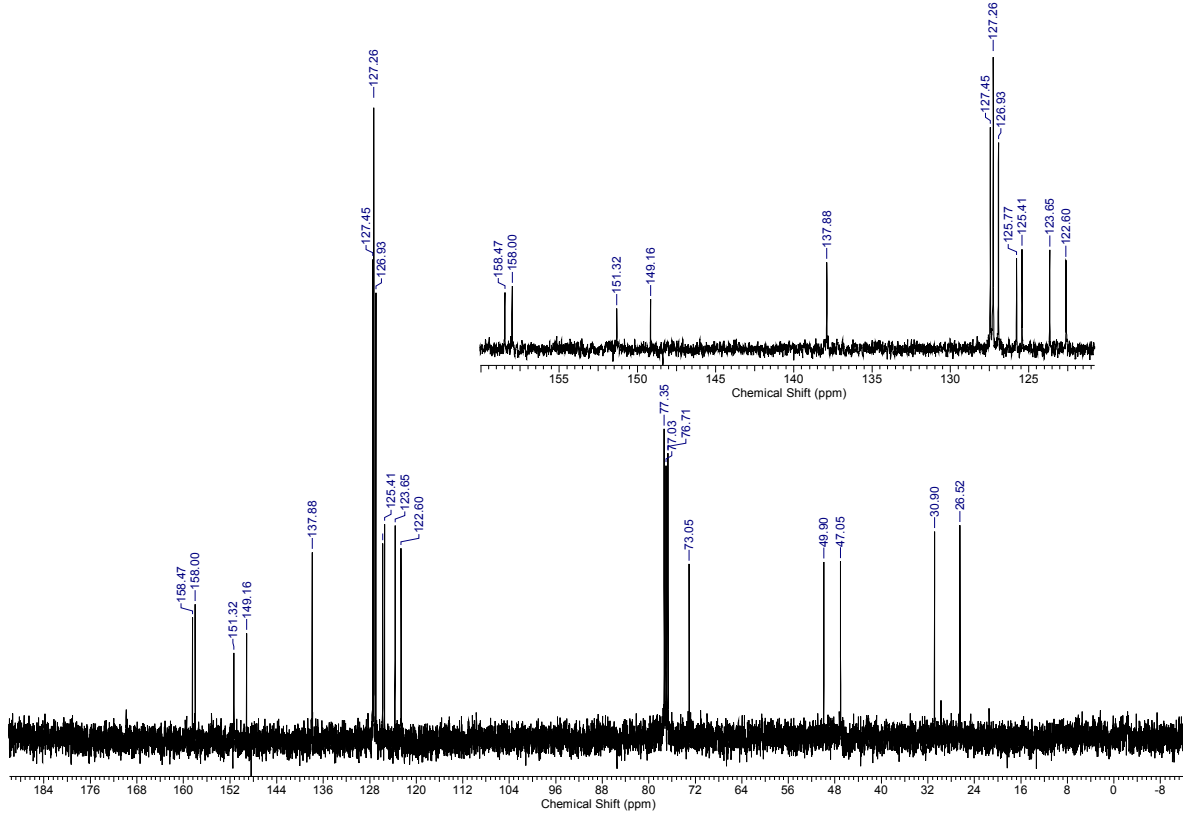


**Figure S16.** <sup>13</sup>C NMR spectrum (CDCl<sub>3</sub>, rt) of complex 3a.

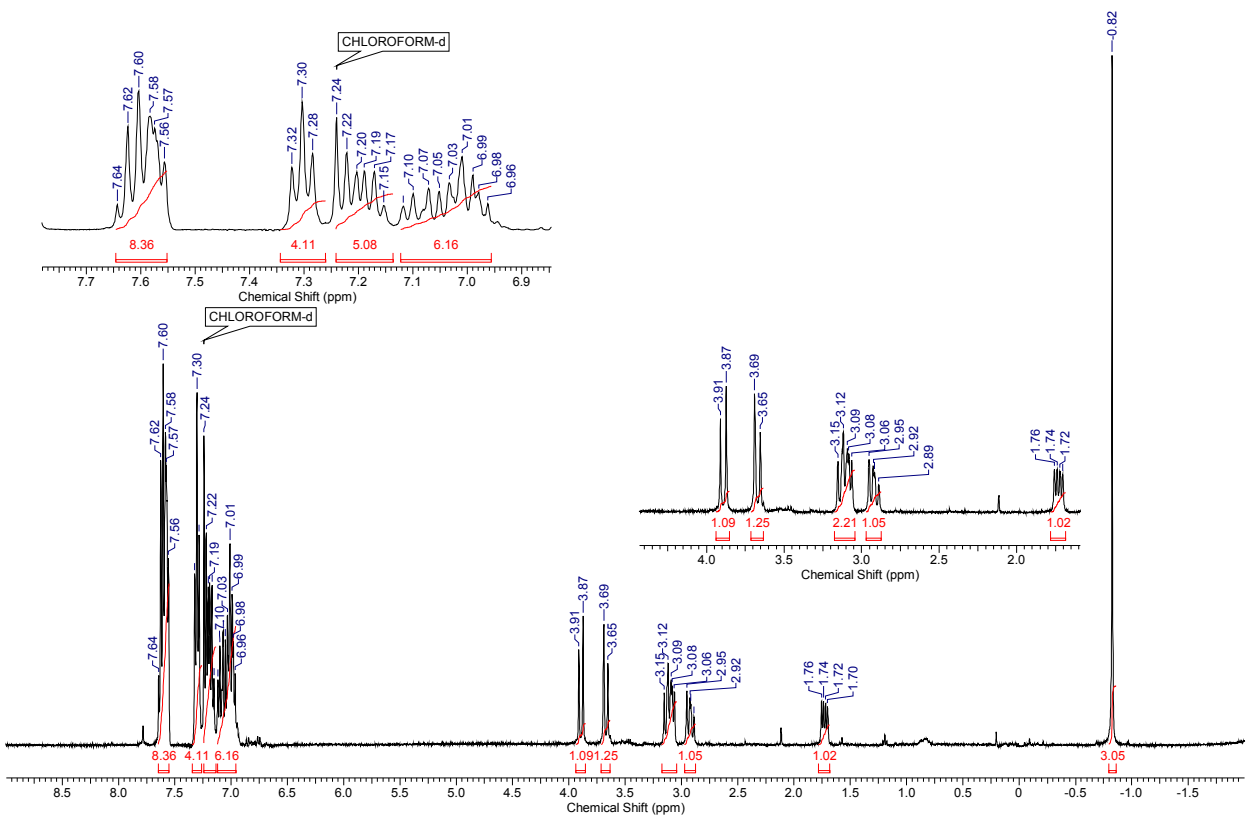


**Figure S17.**  $^1\text{H}$  NMR spectrum ( $\text{CDCl}_3$ , rt) of complex **4a**.

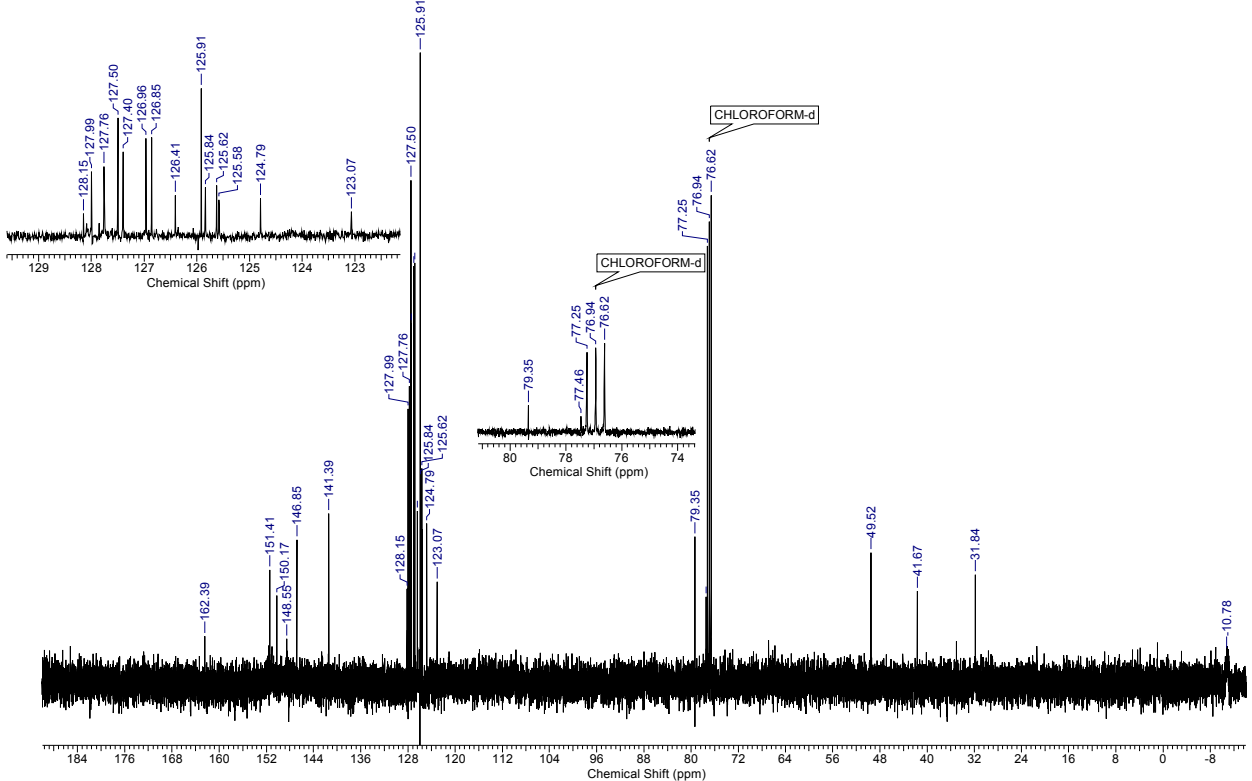


**Figure S18.**  $^{13}\text{C}$  NMR spectrum ( $\text{CDCl}_3$ , rt) of complex **4a**.

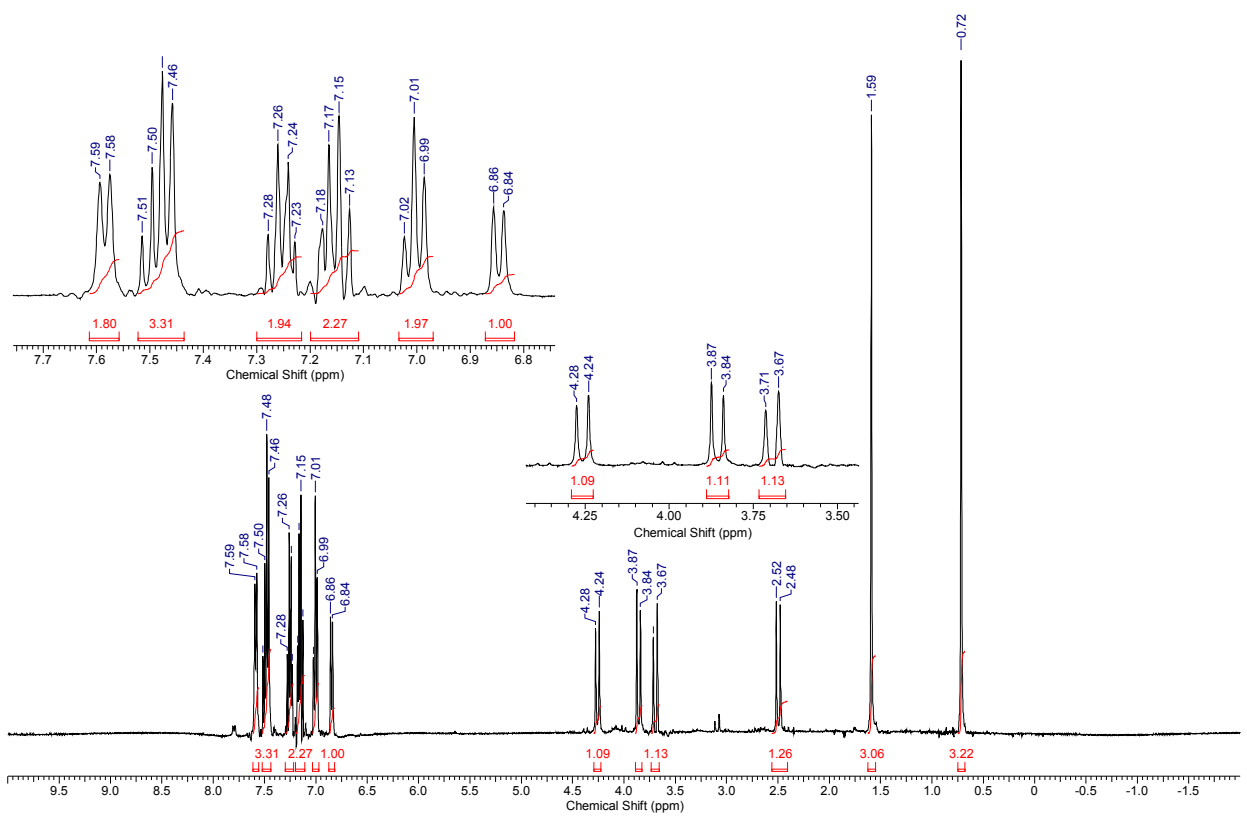


**Figure S19.**  $^{13}\text{C}$  NMR spectrum ( $\text{CDCl}_3$ , rt) of complex **3b**.

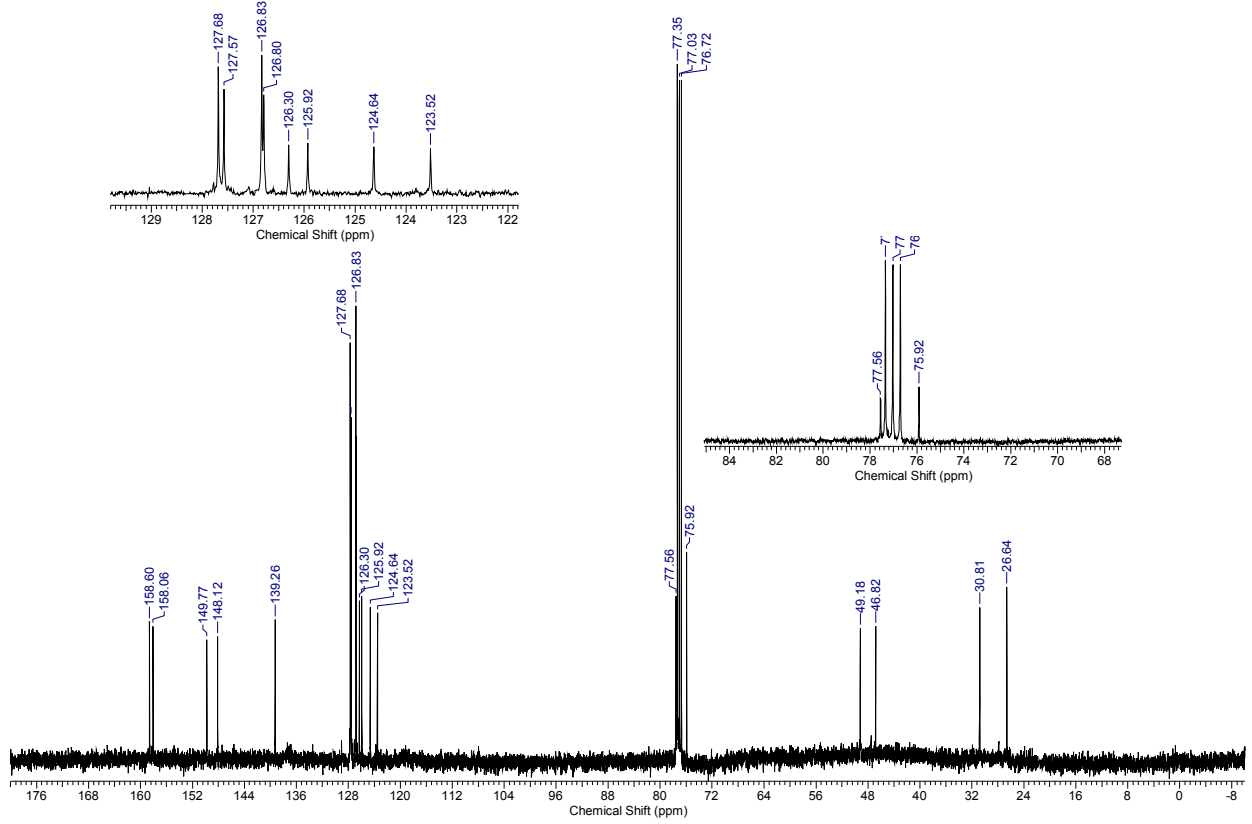


**Figure S20.**  $^{13}\text{C}$  NMR spectrum ( $\text{CDCl}_3$ , rt) of complex **3b**.

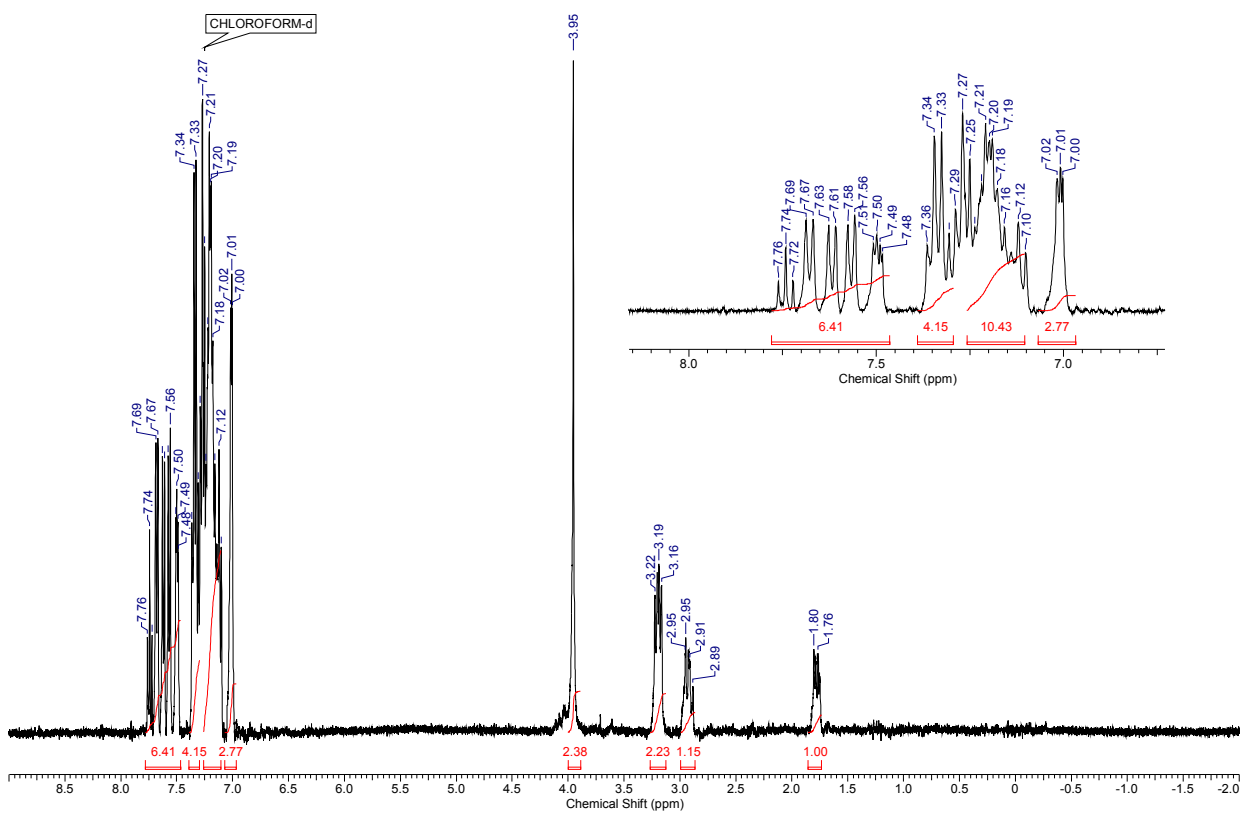


**Figure S21.**  $^1\text{H}$  NMR spectrum ( $\text{CDCl}_3$ , rt) of complex **4b**.

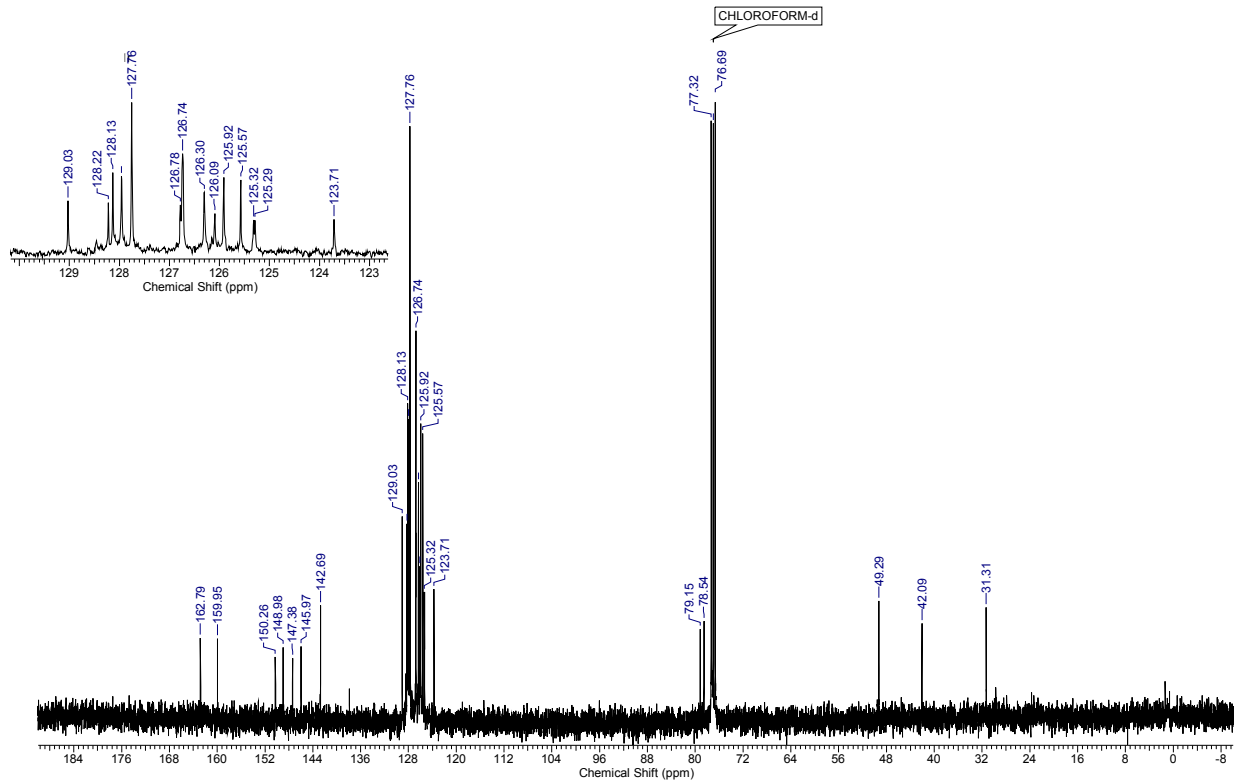


**Figure S22.**  $^{13}\text{C}$  NMR spectrum ( $\text{CDCl}_3$ , rt) of complex **4b**.

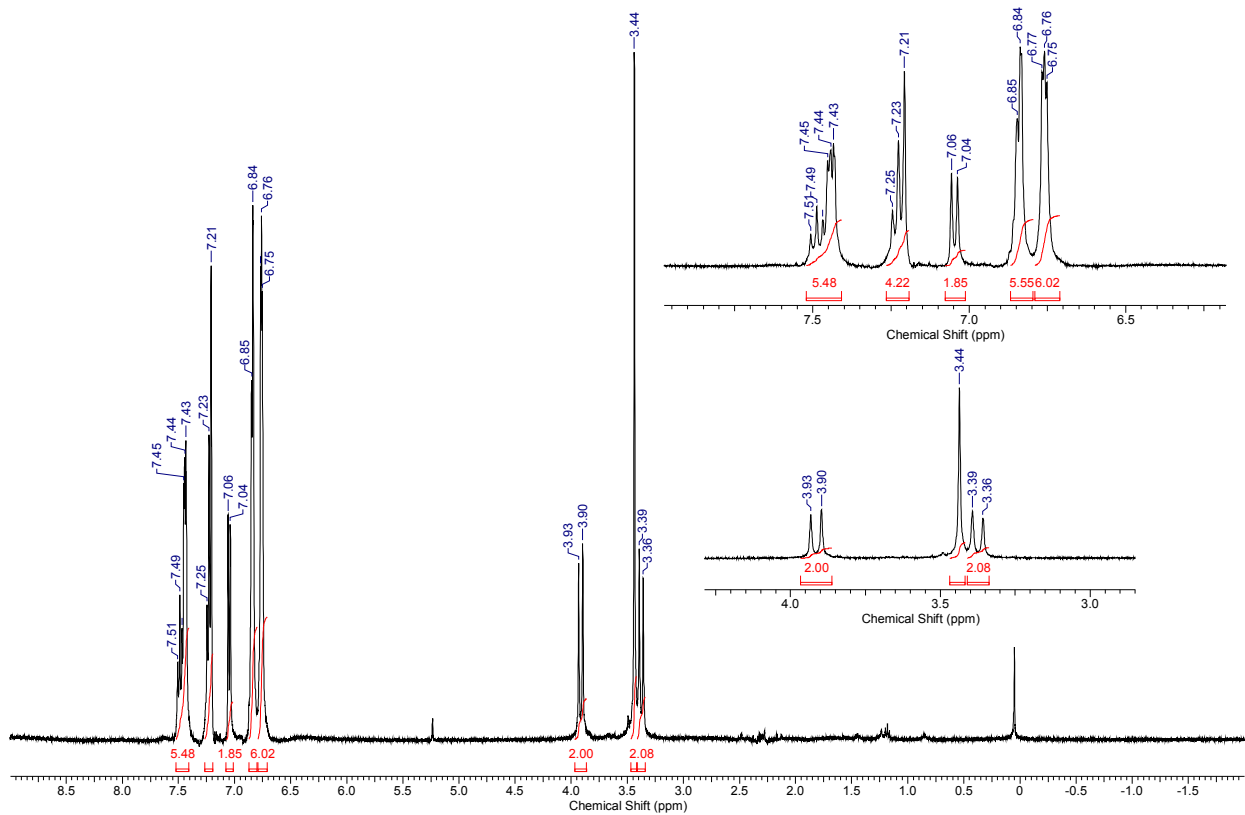


**Figure S23.** <sup>1</sup>H NMR spectrum ( $\text{CDCl}_3$ , rt) of complex **2c**.

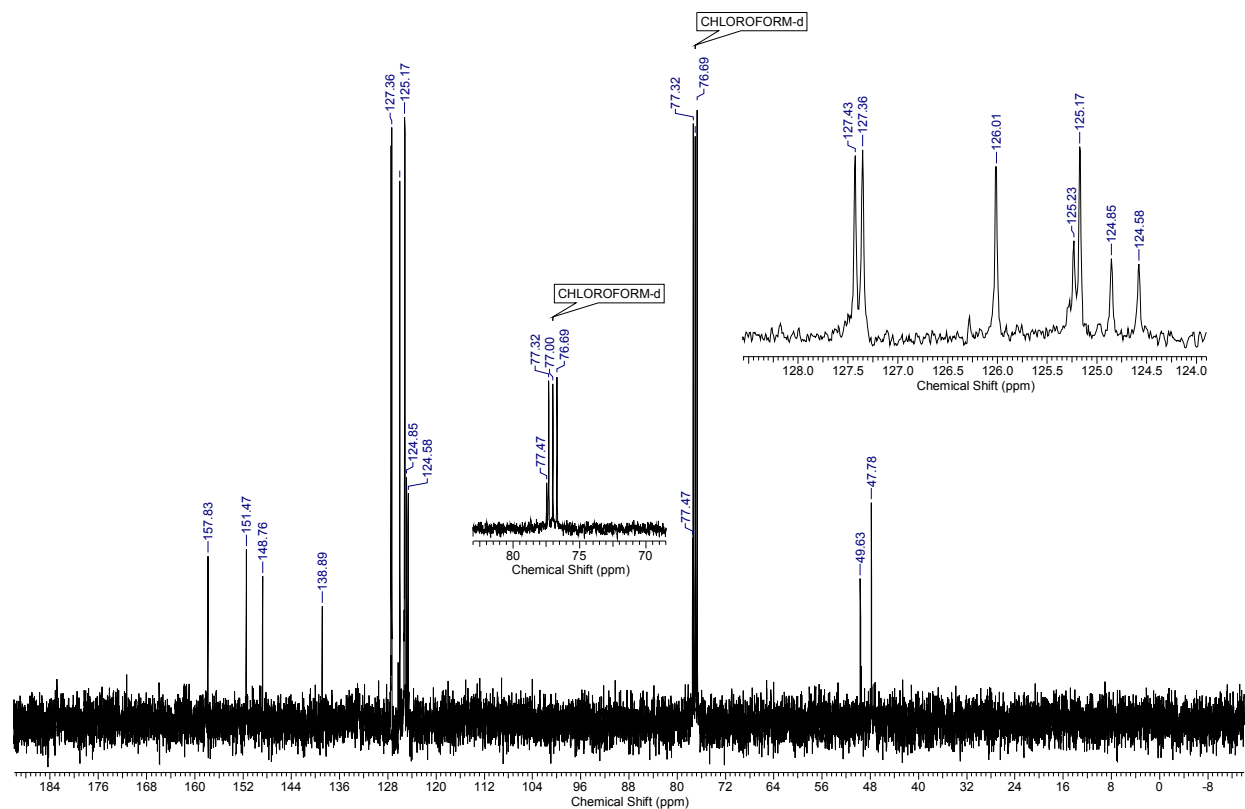


**Figure S24.** <sup>13</sup>C NMR spectrum ( $\text{CDCl}_3$ , rt) of complex **2c**.

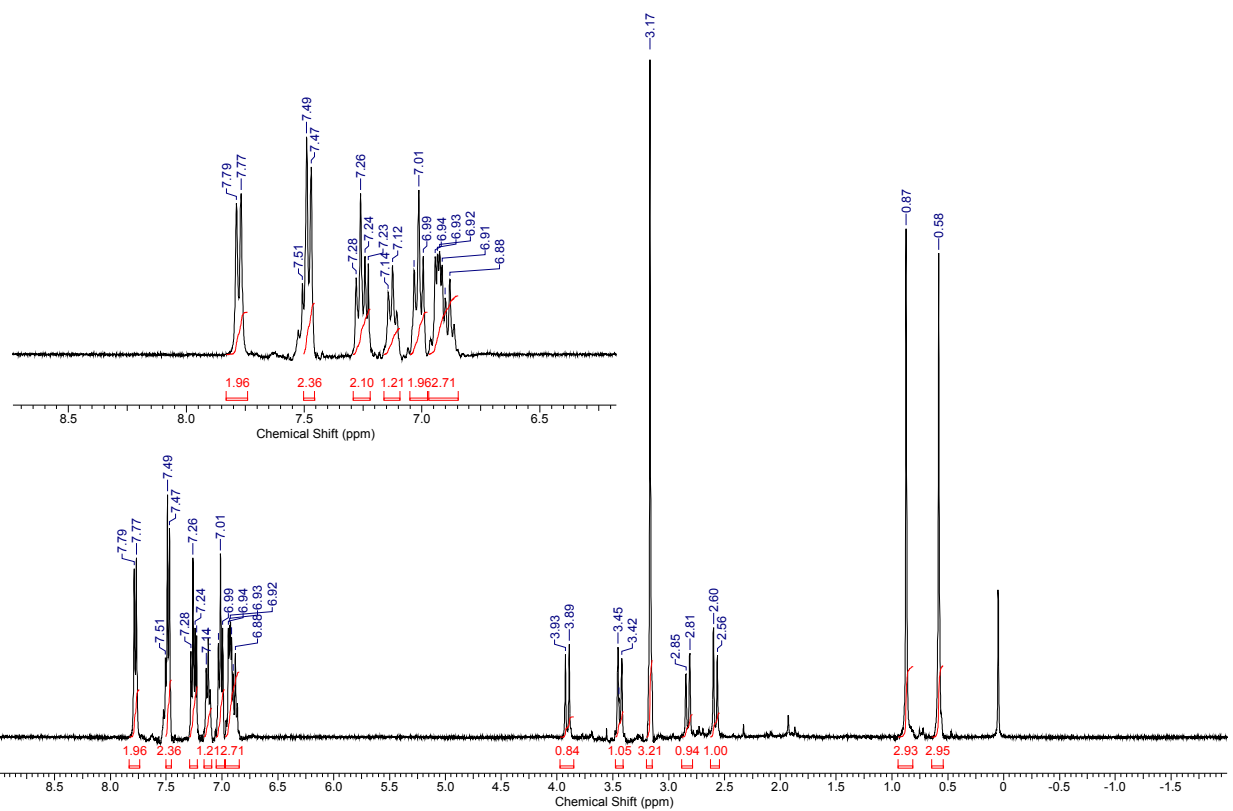


**Figure S25.** <sup>1</sup>H NMR spectrum (CDCl<sub>3</sub>, rt) of complex **3c**.

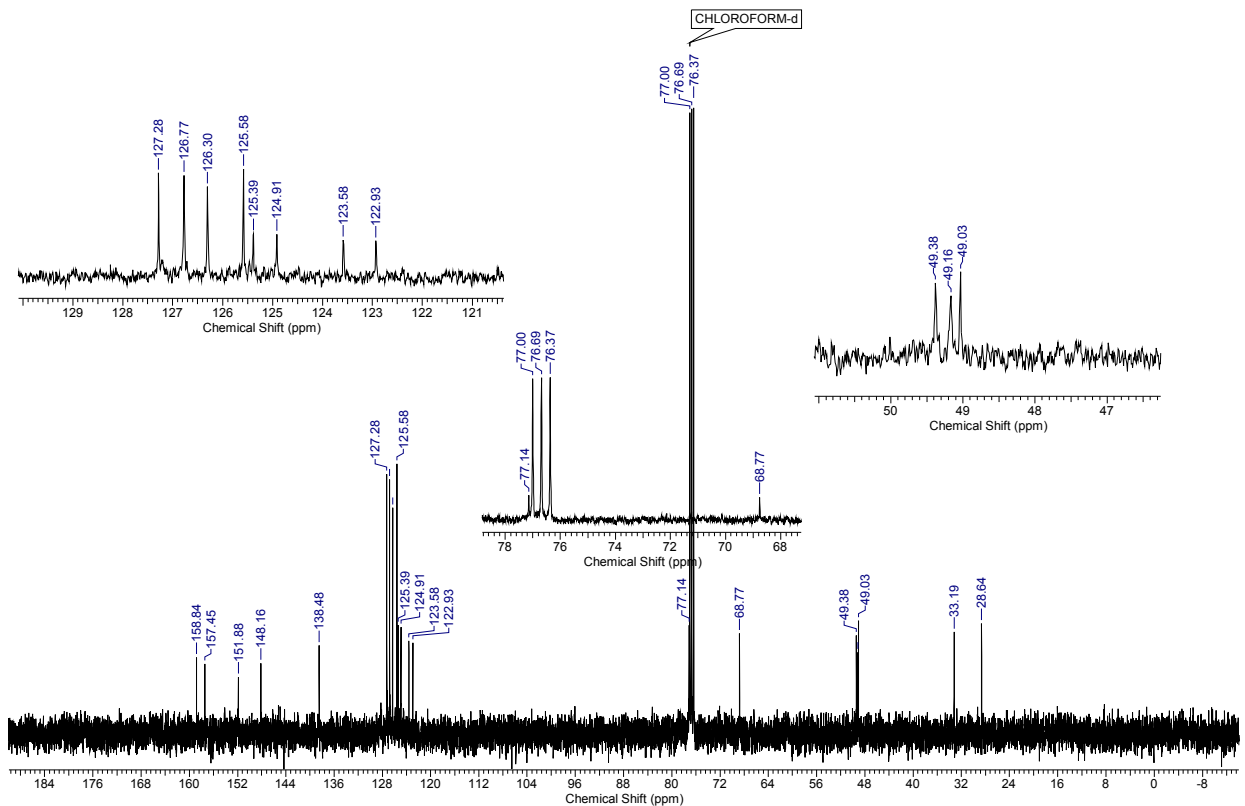


**Figure S26.** <sup>13</sup>C NMR spectrum (CDCl<sub>3</sub>, rt) of complex **3c**.

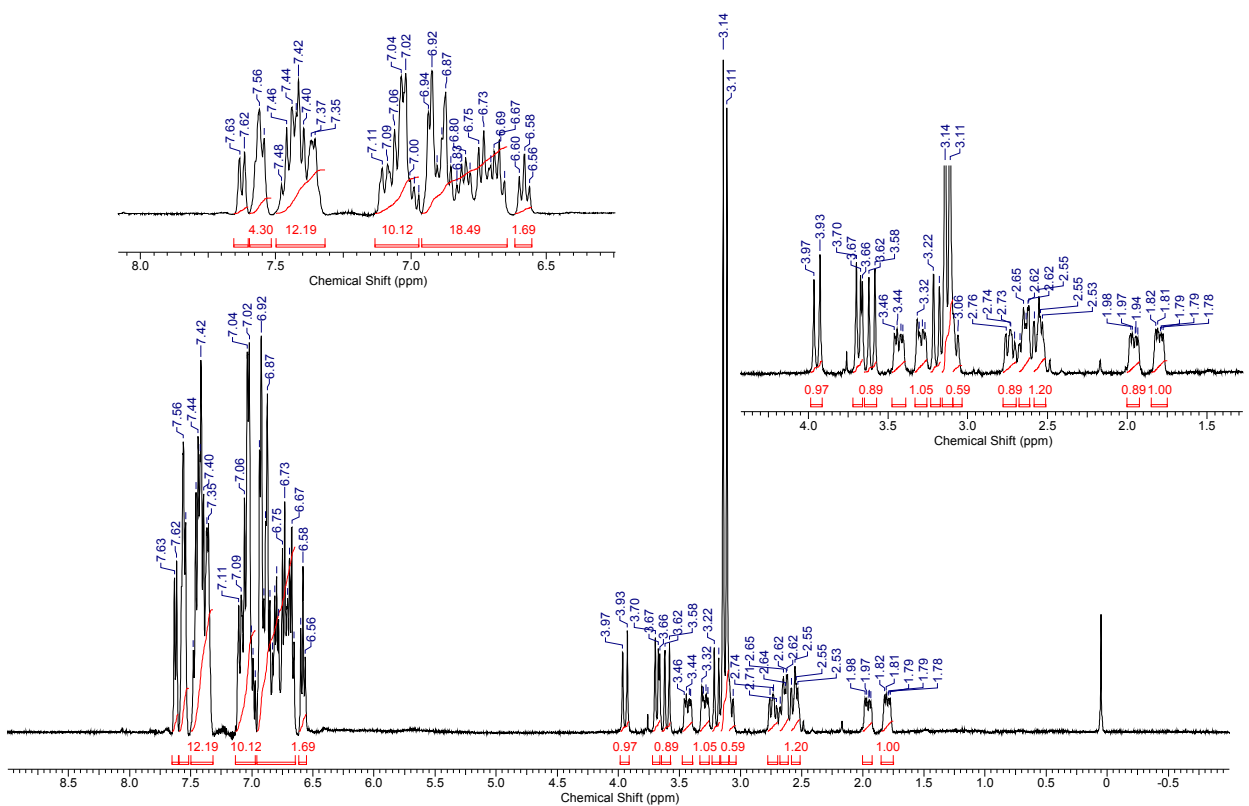


**Figure S27.**  $^1\text{H}$  NMR spectrum ( $\text{CDCl}_3$ , rt) of complex **4c**.

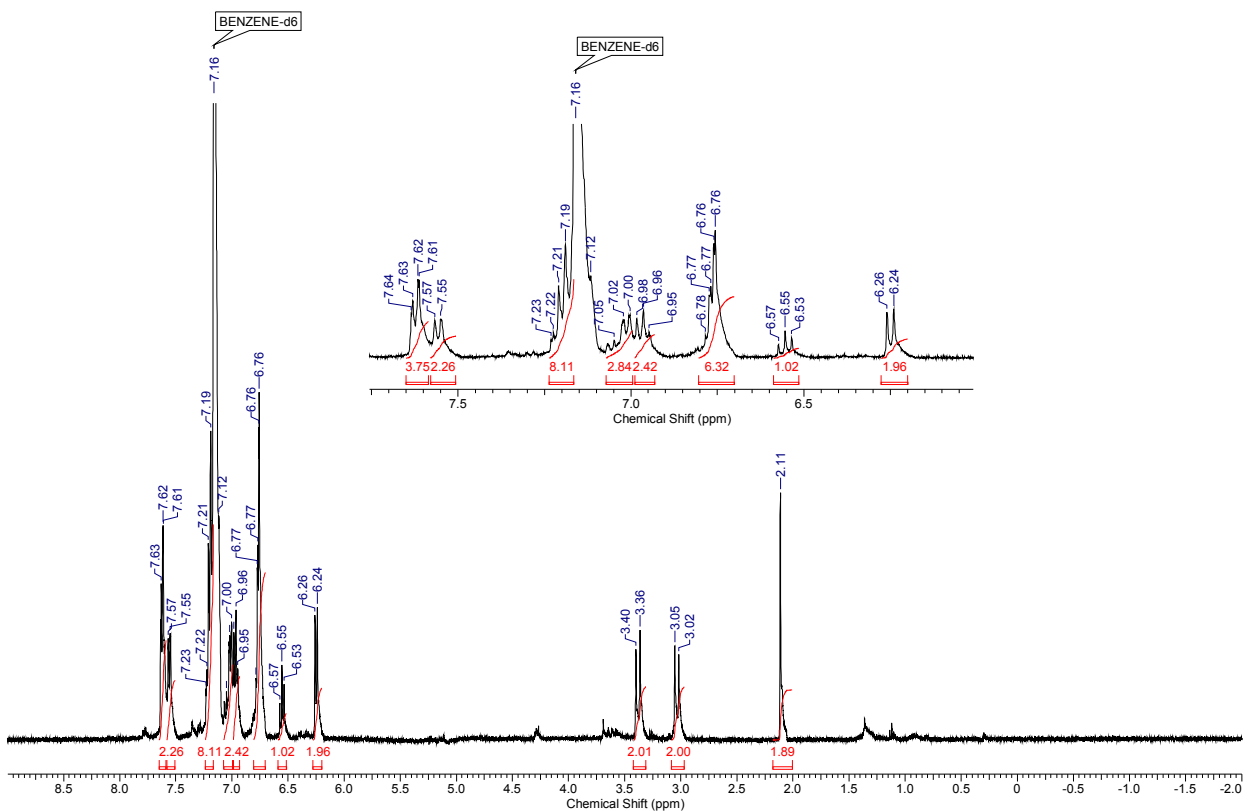


**Figure S28.**  $^1\text{H}$  NMR spectrum ( $\text{C}_6\text{D}_6$ , rt) of complex **2d**.

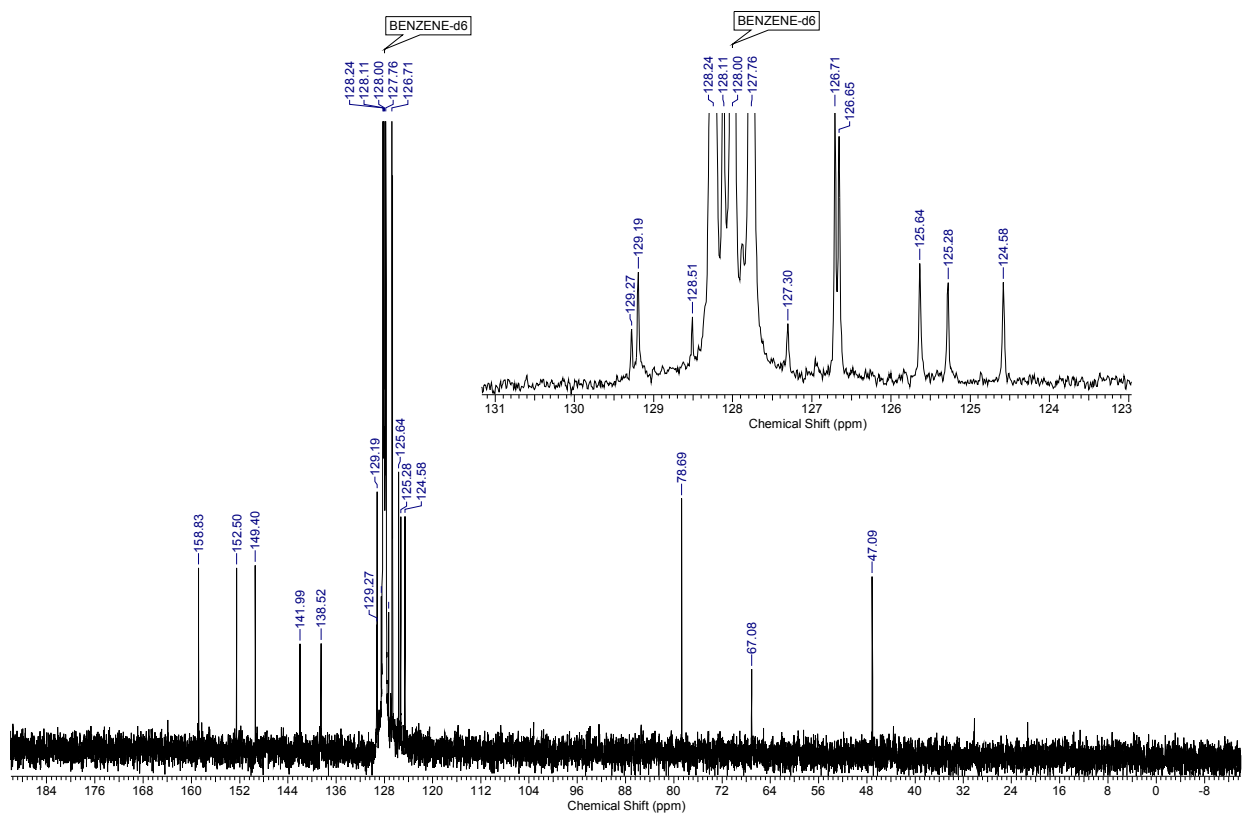


**Figure S29.**  $^{13}\text{C}$  NMR spectrum ( $\text{C}_6\text{D}_6$ , rt) of complex **2d**.